Journal of Hazardous Materials 161 (2009) 1313–1322

Contents lists available at ScienceDirect

Journal of Hazardous Materials

journal homepage: www.elsevier.com/locate/jhazmat

Sorption of distillery spent wash onto fly ash: Kinetics, mechanism, process design and factorial design

R. Krishna Prasad*, S.N. Srivastava

School of Chemical & Biotechnology, SASTRA University, Thanjavur 613402, India

ARTICLE INFO

Article history:
Received 1 February 2008
Received in revised form 23 April 2008
Accepted 23 April 2008
Available online 1 May 2008

Keywords:
Adsorption
Fly ash
Kinetics
Factorial design
Process design

ABSTRACT

Batch and continuous experiments were performed for the sorption of distillery spent wash onto fly ash particles. The Freundlich and pseudo-second order equation were found to fit the equilibrium data perfectly. The Weber–Morris intraparticle diffusion isotherm equation was used to predict the sorption mechanism and the predicted equation for 10% dilution of spent wash sorption is $q_t = 1.1344t^{0.5} + 33.304$. The optimization using 2^3 factorial design of experiments provides optimal removal of color of 93% for dilution (5%), dosage of adsorbent (10 g) and temperature (293 K). The actual color removal at optimal conditions was 92.24%, confirms close to the factorial design results. The complete error analysis using six non-linear error functions: Chi-square (χ^2); sum of square errors (SSE); composite fractional error function (HYBRD); derivative of Marquardt's percent standard deviation (MPSD); average relative error (ARE); sum of absolute errors (EABS) were calculated. Free energy of adsorption at 293 K ($\Delta G^0 = -1574.67$ J), enthalpy change ($\Delta H^0 = -32.5487$ KJ) and entropy change ($\Delta S^0 = 105$ J/K) were calculated to predict the nature of adsorption. Adsorption studies in a packed column were evaluated using Bed depth service time model, Thomas model and Adams–Bohart model.

1. Introduction

The wastewater from molasses based alcohol distilleries is known as molasses spent wash (MSW). When released in aquatic system, it leads to reduction of sunlight penetration in rivers, lakes and thereby reducing the photosynthetic activity. Disposal on land cause reduction in soil alkalinity, manganese availability and inhibits seed germination [1–3].

MSW from distillation still contains nearly 2% of a dark brown recalcitrant pigment called melanoidin formed due to Maillard amino-carbonyl reaction. The empirical formula of melanoidin is $C_{17-18}H_{26-27}O_{10}N$. It is a product of non-enzymatic reaction between sugars and amino compounds. The molecular weight distribution is between 5000 and 40,000. It is acidic, polymeric and composed of highly dispersed colloids, which are negatively charged due to the dissociation of carboxylic acids and phenolic groups [4–6].

Several studies have been carried out concerning the decolorization of waste water using cyanobacterium [7], fungi such as *Aspergillus fumigatus* [8], *Coriolus* [9] and *Phanerochaete chrysosporium* [10] have shown to degrade melanoidin and anaerobic mass imparting color to spent wash. Basically being heterotrophs, these organisms tend to deplete oxygen in the effluent and further, higher fungi are not easily adopted for aquatic habitats.

The application of electrochemical methods is another way to treat wastewaters. This method guarantees high treatment efficiency, but its effectiveness depends on the type of electrodes, the construction of electrocoagulators and the condition under which the process is run [11,12].

The removal of color using coagulation is widely practiced method of removing particulate and organic matter in wastewater treatment. Conventional coagulants in wastewater treatment are alum ($Al_2(SO_4)_3{\cdot}14H_2O$), ferric chloride ($FeCl_3{\cdot}6H_2O$), sodium aluminate, aluminum chloride and ferric sulfate [13–17]. However, recent studies have pointed out that the presence of aluminum salts in the effluent results in environmental problems [18]. There is also the problem of reaction of alum with natural alkalinity present in the water leading to a reduction of pH [19].

Currently sorption technique is proved to be an effective and attractive process for the wastewater treatment. Also this method will become inexpensive, if the sorbent material used is of cheaper cost and does not require any expensive additional pretreatment step. During coal-fired electric power generation, two main types of coal combustion by products are obtained, fly ash and bottom ash. The current annual worldwide production of coal ash is estimated about 700 million tons of which at least 70% is fly ash [20]. Although, significant quantities are being used in a range of applications like substitute for cement in a concrete, however still large

* Corresponding author. Tel.: +91 94434 60815; fax: +91 4362 264120.
E-mail address: rkprasad_cbe@rediffmail.com (R. Krishna Prasad).

0304-3894/$ – see front matter © 2008 Elsevier B.V. All rights reserved.
doi:10.1016/j.jhazmat.2008.04.092

Nomenclature

ANOVA	analysis of variance
ARE	average relative error
$1/b_T$	adsorption potential (KJ/mol)
B_t	Boyd number which is a mathematical function of F
C_b	column break through concentration (mg/dm^3)
C_e	equilibrium concentration in liquid phase (mg/dm^3)
C_t	concentration of spent wash solution at time t (mg/dm^3)
C_0	initial concentration of spent wash solution (mg/dm^3)
D	adsorbent dosage (g/dm^3)
D_i	effective diffusion coefficient (cm^2/s)
EABS	sum of absolute errors
F	fraction of solute adsorbed at any time t
ΔG^0	Gibbs free energy change (J/mol)
HYBRD	composite fractional error function
ΔH^0	change in enthalpy (J/mol)
I	integral constant
K_a	bed depth service time model constant (L/mg min)
K_f	Freundlich constant (mg/g) (dm^3/mg)$^{1/n}$
K_i	intraparticle diffusion rate constant (mg/g min$^{0.5}$)
K_{AB}	kinetic constant in the Adams–Bohart model (L/mg min)
K_L	Langmuir adsorption constant (dm^3/mg)
K_T	sorption equilibrium constant
K_{Tem}	Temkin isotherm constant (dm^3/g)
K_{Th}	Thomas model constant (L/mg min)
K_1	pseudo-first order rate constant (min^{-1})
K_2	pseudo-second order rate constant (g/mg min)
m_{total}	total amount of solids sent to the column (mg)
M	amount of adsorbent (g)
MPSD	derivative of Marquardt's percent standard deviation
$1/n$	Freundlich parameter
N_0	sorption capacity of the bed per unit volume of the bed (mg/L)
P	smallest level of significance leading to rejection of null hypothesis
q	amount of spent wash adsorbed at any time (mg/g)
q_e	equilibrium concentration in solid phase (mg/g)
q_m	Langmuir isotherm parameter, maximum spent wash adsorbed/unit mass of adsorbent (mg/g)
q_o	amount of spent wash adsorbed at infinite time (mg/g)
q_t	amount of spent wash adsorbed per unit mass of adsorbent at time t (mg/g)
Q	column feed flow rate (ml/min)
r	radius of particle calculated assuming spherical size (cm)
r^2	linear regression correlation coefficient
R	universal gas constant (8.314 J/mol K)
R_L	Langmuir separation or equilibrium parameter (dimensionless)
$\%R_t$	percentage color removal
SSE	sum of square errors
ΔS^0	change in entropy (J/mol K)
t	time (min)
t_b	column service time corresponding to break through concentration (min)
t_{total}	total flow time (min)
T	temperature (K)
U_0	superficial velocity of the solution (cm/min)
V	volume of spent wash (L)
V_{eff}	effluent volume (ml)
q_{total}	total adsorbed quantity in the column (mg)
Z	bed height (cm)
χ^2	Chi-square

amounts are not used and this requires disposal. Making a more productive use of fly ash would have considerable environmental benefits, reducing air and water pollution. The large amount of fly ash discarded in coal-fired power stations can be utilized as a good adsorbent for color removal [21–24]. Previously several researchers had proved several low cost materials such as rice husk [25], wheat shell [26], bagasse pith [27] were used in color removal. Scrap rubber, peanut husks and composted bark to remove metal ion from wastewater [28,29]. The adsorbent capacity of reactive dyes on the fly ash particles of 45 μm size for adsorbent dosage 500 mg/L for remazol red (129 mg/g), remazol blue (17 mg/g) and rifacion yellow (28 mg/g). The adsorbent capacity for 56.5 μm particle size are 114 mg/g, 13 mg/g and 25 mg/g for remazol red, remazol blue and rifacion yellow, respectively [24]. This illustrates good adsorption potential of fly ash in sorption of colored compounds and can be utilized in decolorization of spent wash. Thus, the fly ash can be used as effective adsorbent to remove the color from textiles, dye effluent apart from distillery spent wash.

In the present study, the effects of adsorbent dosage, pH, particle size, dilution of spent wash and temperature were studied. The data were treated with five types of isotherm models to determine the best-fit model for batch adsorber design. Further the sorption mechanism was analyzed using intraparticle diffusion studies. Apart from complete error analysis using six different types of non-linear error functions, thermodynamic models were also developed. In order to study the combined effects of important factors affecting the adsorption and to optimize the set of factors the 2^3 factorial design models were developed. Packed bed adsorption studies were also conducted and the results were analyzed using Thomas model and Adams–Bohart model.

2. Experimental materials and methods

The spent wash used for the study was collected from a distillery unit near Tiruchi in Tamil Nadu, India. The sample was diluted to desired dilution using deionized water. The pH of the sample was adjusted using 0.1 M H_2SO_4 or 0.1 M NaOH as required. Table 1 gives the physico-chemical characteristics of raw spent wash analyzed as described in standard methods [30].

Table 1
Physico-chemical characteristics of distillery spent wash (10% diluted)

Parameters	Magnitude
pH	4.2–4.3
Temperature (°C)	30
Color	Dark brown
Initial absorbance	1.733
Odor	Burnt sugar
Chemical oxygen demand (mg/L)	10000–11000
Biochemical oxygen demand (mg/L)	7000–7500
Total dissolved solids (mg/L)	5500–5700
Chloride (mg/L)	500–600
Potassium (mg/L)	1000–1300
Calcium (mg/L)	210–300

The fly ash was obtained from Neyveli Lignite Thermal Power Station at Neyveli. The fly ash was sieved by using a sieve set and then was collected in the range of BSS # −72 + 100, −100 + 150, −150 + 200 and −200 + 300 mesh size with corresponding average diameter 0.1815, 0.128, 0.09 and 0.071 mm, respectively. The fly ash was used as received without any pretreatment in the adsorption experiments. Chemical composition of fly ash by chemical analysis was given as SiO_2, 15.14; Fe_2O_3, 3.30; Al_2O_3, 7.82; CaO, 24.66; MgO, 4.5;SO_3, 14.22; K_2O, 0.28;Na_2O, 0.57 and TiO_2, 1.03 and loss on ignition, 2.31 wt%.

2.1. Batch studies

Batch adsorption studies were conducted by varying adsorbent dosage, particle size, pH, initial dilution and temperature. In each experiment accurately weighed fly ash was added to 100 cm^3 of distillery spent wash solution taken in a 250 cm^3 conical flask and the mixture was agitated at 200 rpm in an incubated shaker at constant temperature. The analysis of sample was done after filtering it using Whatmann 42 filter paper. Concentrations of the filtered samples were determined from the absorbance of the solution at the characteristic wavelength 475 nm using a double beam UV–vis spectrophotometer (Systronics 2201) [31,5]. The readings were taken in duplicate for each individual solution to check repeatability and the average of the values were taken.

Percentage color removal (R_t) was calculated using the formula

$$\%R_t = \frac{(C_0 - C_t)}{C_0} \times 100 \quad (1)$$

Specific uptake was calculated by

$$q_t = \frac{(C_0 - C_t)}{D} \quad (2)$$

2.2. Continuous studies

Bulk removal of spent wash onto fly ash was investigated using packed bed of BSS # −100 + 150 mesh size fly ash particles. Glass column with internal diameter 2 cm, fitted with five sampling points at 5 cm intervals, was used for the study. At the bottom of the packing 2 cm high layer of glass beads (3 mm diameter) was used to provide uniform inlet flow to the column. Distillery spent wash solution was introduced into the column at desired flow rate using a peristaltic pump. Samples were collected at regular intervals from all the sampling points. The performance of packed column is described through the concept of the breakthrough curve, which is the plot of time versus effluent concentration curve.

2.3. Factorial design

The factorial design helps to develop a statistical model of a reaction by performing the minimum number of well-chosen experiments and to determine the optimal values of process parameters. Factorial design is an empirical modeling technique used to evaluate the relationship between experimental variables and corresponding responses. The design of experiments chosen for this study was the 2^3 factorial design for three independent variables dilution (X_1), dosage of adsorbent (X_2) and temperature (X_3).

The behavior of the system is explained by the following quadratic equation [32,33].

$$Y = b_o + b_1X_1 + b_2X_2 + b_3X_3 + b_4(X_1X_2) + b_5(X_2X_3) + b_6(X_1X_3) + b_7(X_1X_2X_3) \quad (3)$$

where b_o represents the global mean and b_i represents the regression coefficient corresponding to the main factors effects and interactions.

The results of experimental design were studied and interpreted by MINITAB 14 statistical software to estimate the response of dependent variable (% color removal).

3. Results and discussions

3.1. Effects of different factors on adsorption process

Fig. 1 indicates the effect of amount of sorbent utilized on %color removal of distillery spent wash at pH 7 and reaction temperature of 303 K. Color removal increased very rapidly by increasing the amount of sorbent from 2 g to 14 g. The color removal reached maximum of 91% for 10 g sorbent. Further increase in sorbent dosage was found ineffective for increasing the color removal beyond this level. The color removal decreased slightly at dosage beyond 10 g that may be attributed to interference of fly ash particles itself beyond equilibrium color removal. The color removal increased with increase in sorbent dosage due to increased availability of surface area for adsorption.

The specific surface area available for adsorption increases with decrease in particle size of sorbent. The studies were conducted at four different particle sizes of BSS # −72 + 100, −100 + 150, −150 + 200 and −200 + 250 with corresponding average diameter 0.1815, 0.128, 0.09, 0.071 mm, respectively. Fig. 2 indicates that maximum color removal of 93% obtained for −150 + 200 particle size and further reduction in particle size does not contribute much for increase in color removal.

The effect of pH on color removal is shown in Fig. 3 for the range of pH 2–11. The color removal was more than 87% for pH range 2–7. This provides that acidic and neutral pH is effective for adsorption

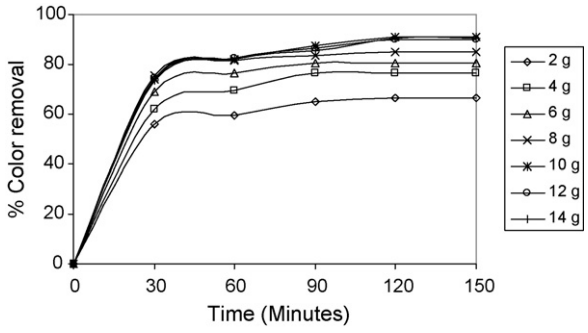

Fig. 1. Effect of fly ash dosage on %color removal. (Conditions: pH 7: dilution = 10%; temperature = 303 K; particle size BSS # −100 + 150).

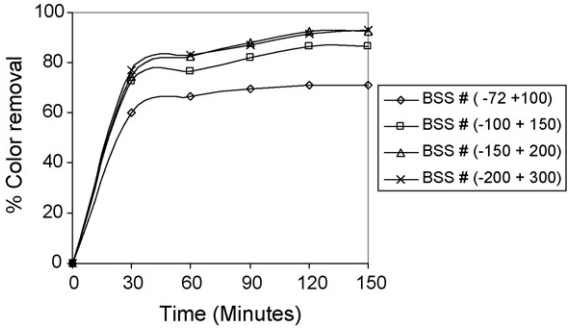

Fig. 2. Effect of particle size on %color removal. (Conditions: pH 7; dilution = 10%; temperature = 303 K; dosage = 10 g).

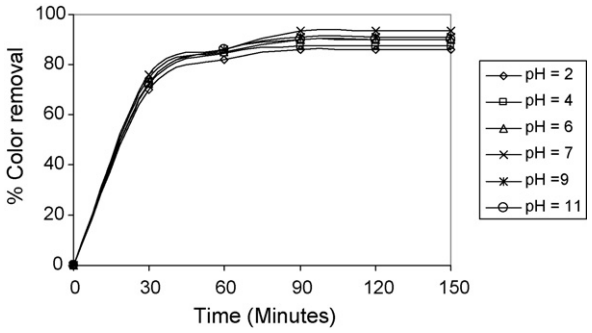

Fig. 3. Effect of pH on %color removal. (Conditions: dilution = 10%; temperature = 303 K; particle size (BSS) # −150 + 200; dosage = 10 g).

of spent wash than alkaline pH range. However for convenience of treatment of effluent to meet the standards of pollution control board the optimized pH was fixed at 7 for further studies.

The temperature is one of the most important factors that affect the adsorption rate. The effect of temperature on the adsorption of spent wash onto fly ash was studied at different initial concentrations of spent wash. The initial concentrations of spent wash are 2000, 5500, 8700 and 12500 mg/L for 5%, 10%, 15% and 20% dilution, respectively. Other parameters were maintained constant (pH 7, dosage of 10 g and particle size BSS # −150 + 200). The increase in temperature decreases the rate of adsorption as at higher temperature sorbate adsorption into pores of sorbent is ineffective due to chance of desorption of sorbate at higher temperatures.

3.2. Adsorption isotherms

The prediction of batch sorption kinetics is necessary for the design of industrial sorption columns. The nature of the sorption process will depend on physical or chemical characteristics of the adsorbent system and also on the system conditions. The results of the studies conducted were analyzed using five different isotherm models. Six different non-linear error functions χ^2, SSE, HYBRD, MPSD, ARE, EABS and linear error function r^2 were employed to find out the most suitable isotherm models. The definition of these error functions was described elsewhere [34,35].

Freundlich sorption isotherm is most widely used empirical expression that accounts for the surface heterogeneity, exponential distribution of active sites of sorbent and their energies towards sorbate. The empirical model can be represented as [36]:

$$q_e = K_f C_e^{1/n} \tag{4}$$

The linearized form of Freundlich isotherm is given as follows.

$$\ln q_e = \ln K_f + \frac{1}{n} \ln C_e \tag{5}$$

A plot of $\ln q_e$ versus $\ln C_e$ yields a straight line, with a slope of $1/n$ and intercept of $\ln K_F$. The value of n should lie in the range of 1–10 for favorable adsorption.

Langmuir isotherm model was originally developed to represent monolayer sorption on a set of distinct localized sorption sites. It gives uniform energies of monolayer sorption onto sorbent surface with no transmigration of sorbate in the plane of the surface. There are no interaction between sorbed molecules, no steric hindarance between sorbed molecules and incoming ions. It is represented as [37]:

$$q_e = \frac{(q_m K_L C_e)}{(1 + K_L C_e)} \tag{6}$$

The linearized form of Langmuir isotherm:

$$\frac{1}{q_e} = \frac{1}{K_L q_m C_e} + \frac{1}{q_m} \tag{7}$$

The plot of $1/q_e$ versus $1/C_e$ yields a straight line.

The essential characteristics of the Langmuir isotherm can be expressed in terms of dimensionless constant separation factor or equilibrium parameter, R_L, given by

$$R_L = \frac{1}{(1 + K_L C_0)} \tag{8}$$

The parameter R_L indicates the shape of isotherm ($R_L > 1$ isotherm is unfavorable, $R_L = 1$ it is linear, $0 < R_L < 1$ it is favorable and $R_L = 0$ it is irreversible).

The Temkin isotherm was studied to explore the energy distribution pattern. The Temkin isotherm has been expressed in the following form [38]:

$$q_e = \left(\frac{RT}{b_T}\right) \ln (K_{Tem} C_e) \tag{9}$$

The linear form of Temkin isotherm model is

$$q_e = \left(\frac{RT}{b_T}\right) \ln K_{Tem} + \left(\frac{RT}{b_T}\right) \ln C_e \tag{10}$$

The Freundlich isotherm fits to the experimental equilibrium data with value of n as 2, which lies within 1–10 for favorable adsorption. Moreover, the r^2 value is 0.9998, which is larger than that of Langmuir isotherm (0.9874) and Temkin isotherm (0.95463). The predicted equation using Freundlich parameters is:

$$q_e = 1.5931 C_e^{0.4962} \tag{11}$$

The values of R_L using Langmuir adsorption at lower concentration of 5% dilution is 0.20507, which lies in the range of 0–1 indicating favorable adsorption process at lower concentration. But as initial concentration increased the R_L values decreases (R_L value is 0.08576 for 10% dilution, 0.055987 for 15% dilution and 0.03964 for 20% dilution) indicates that adsorption decreased with increase of initial concentration. The predicted equation using Langmuir parameters is:

$$q_e = \frac{(0.16529 C_e)}{(1 + 0.001938 C_e)} \tag{12}$$

The predicted design equation using Temkin isotherm parameters useful for batch adsorber design is:

$$q_e = 49.705 \ln\ (0.15619 C_e) \tag{13}$$

3.3. Adsorption kinetics

Lagergren pseudo-first order kinetics based on solid capacity originally gives the pseudo-first order kinetic model as follows [39].

$$\frac{dq_t}{dt} = K_1 (q_e - q_t) \tag{14}$$

Integrating for the boundary conditions $t = 0$ to $t = t$ and $q_t = 0$ and $q_t = q_e$ gives

$$\ln(q_e - q_t) = \ln q_e - \frac{(K_1 t)}{2.303} \tag{15}$$

Values of q_e and K_1 can be obtained from the slope and intercept of the plot $\ln (q_e - q_t)$ versus $t/2.303$.

Ho pseudo-second order kinetics data were further analyzed by second order model, which is represented by [40,41]

$$\frac{dq_t}{dt} = K_2 (q_e - q_t)^2 \tag{16}$$

Table 2
Pseudo-first order and pseudo-second order rate constant for the sorption of spent wash onto fly ash

Initial dilution (%)	$q_{e\,(expt)}$	First order model			Second order model		
		$q_{e\,pre}$	K_1	r_1^2	$q_{e,pre}$	K_2	r_2^2
5	18.575	9.370	0.042	0.816	19.027	0.0098	0.995
10	46.327	23.316	0.057	0.883	47.204	0.0053	0.997
15	67.721	48.453	0.042	0.956	69.492	0.0026	0.995
20	90.468	62.219	0.044	0.945	92.465	0.0023	0.996

Table 3
Predicted pseudo-first order and pseudo-second order equation for sorption of spent wash onto fly ash

Initial dilution (%)	Predicted pseudo-first order equation	Predicted pseudo-second order equation
5	$q_t = 9.370 - 9.370/\exp^{0.042t}$	$q_t = t/(3.4349 + t/19.0272)$
10	$q_t = 23.316 - 23.316/\exp^{0.057t}$	$q_t = t/(12.0171 + t/47.20452)$
15	$q_t = 48.453 - 48.453/\exp^{0.042t}$	$q_t = t/(12.9617 + t/69.49284)$
20	$q_t = 62.219 - 62.219/\exp^{0.044t}$	$q_t = t/(20.3572 + t/92.46552)$

Integrating for the boundary conditions $t = 0$ to $t = t$ and $q_t = 0$ and $q_t = q_e$ gives

$$\frac{t}{q_t} = \frac{1}{K_2 q_e^2} + \frac{t}{q_e} \quad (17)$$

Values of q_e and K_2 can be obtained from the slope and intercept of plot t/q_t versus t.

The isotherm parameters of pseudo-first order and pseudo-second order isotherms are given in Table 2. The predicted equations useful for batch adsorber design are given in Table 3.The value of linear correlation coefficient r^2 for Lagergren model is 0.9 which is lower than the r^2 value (0.9962) calculated for Ho's second order model. Fig. 4 provides the equilibrium curve comparing experimental q_e and the predicted values of q_e using various design equations obtained for Freundlich, Langmuir, Temkin, Lagergren and Ho plotted against C_e values.

3.4. Adsorption mechanisms

Though kinetic and equilibrium isotherm studies help to identify the sorption process, predicting the mechanisms is required for design purposes. The external mass transfer (boundary layer diffusion) or intraparticle diffusion or both can characterize the solid–liquid sorption process. The following three steps can describe the sorption dynamics.

- Transfer of the solute from bulk solution through liquid film to the adsorbent exterior surface.
- Solute diffusion into the pore of adsorbent except for a small quantity of sorption on the external surface; parallel to this is the intraparticle transport mechanism of the surface diffusion.
- Sorption of the solute on the interior surface of the pores and capillary spaces of adsorbent.

Of the three steps, the third step is assumed to be rapid and considered to be negligible. The most commonly used technique for identifying the mechanism is by fitting the experimental data in an intraparticle diffusion plot. Previous studies by various researchers showed that the plot of q_t versus $t^{0.5}$ represents multi linearity, which characterize the two or more steps involved in the sorption process. Weber and Morris intraparticle relation is given by

$$q_t = K_i t^{0.5} + I \quad (18)$$

The plot q_t versus $t^{0.5}$ is given by multiple linear regions representing the external mass transfer followed by intraparticle or pore diffusion as represented in Fig. 5.

The two phases in the intraparticle diffusion plot shown in Fig. 5 suggest that the sorption process proceeds by surface sorption and intraparticle diffusion. The initial curved portion of the plot indicates a boundary layer effect while second linear layer is due to intraparticle diffusion or pore diffusion. The calculated intraparticle diffusion coefficients K_i are 0.5832, 1.1344, 2.1463, 2.4762 (mg/g min$^{0.5}$) and r^2 values 0.968, 0.954, 0.953, 0.948 for initial concentration 2000, 5500, 8700 and 12500 mg/L, respectively. The predicted design equations using intraparticle diffusion studies are given in Table 4.

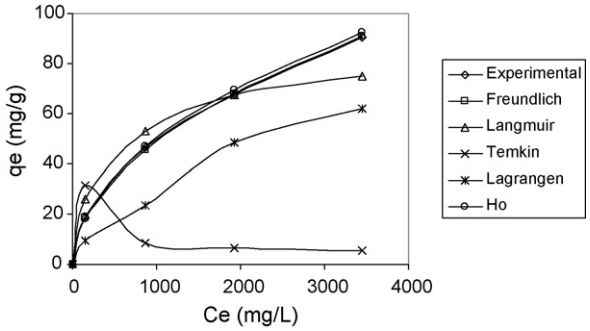

Fig. 4. Comparison of kinetic models in predicting q_e for spent wash sorption onto fly ash (Conditions: temperature = 303 K, pH 7, particle size BSS # −150 + 200, dosage = 10 g; time = 150 min).

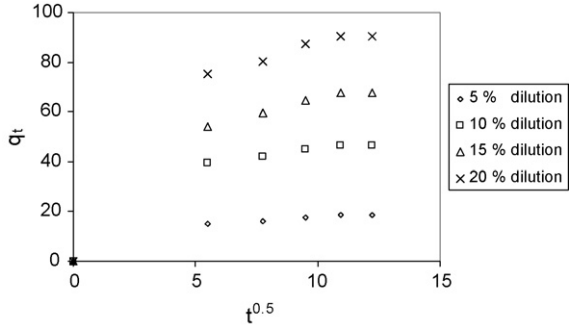

Fig. 5. Weber and Morris intraparticle diffusion plot for sorption of spent wash onto fly ash (Conditions: temperature = 303 K; dosage = 10 g; particle size BSS # −150 + 200, pH 7).

Table 4
Predicted design equation using intraparticle diffusion equation for sorption of spent wash onto fly ash

Initial dilution (%)	Predicted intraparticle diffusion equation
5	$q_t = 0.5832t^{0.5} + 11.796$
10	$q_t = 1.1344t^{0.5} + 33.304$
15	$q_t = 2.1463t^{0.5} + 43.075$
20	$q_t = 2.4762t^{0.5} + 62.007$

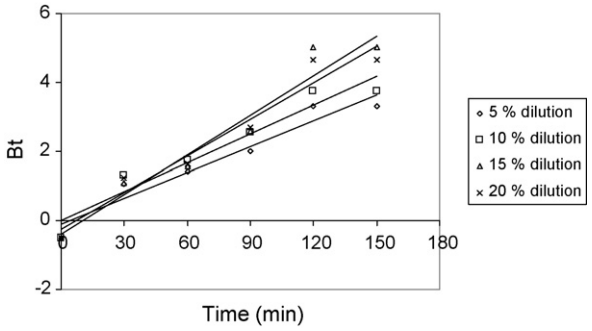

Fig. 6. Boyd kinetic plot (Conditions: temperature = 303 K; dosage = 10 g; particle size BSS # −150 + 200, pH 7).

In order to predict the actual slow step involved, the kinetic data were further analyzed using the Boyd kinetic expression. This kinetic expression predicts the actual slowest step involved in the sorption process for different sorbent sorbate systems.

The Boyd kinetic expression is given by

$$F = 1 - \frac{6}{\pi^2}\exp\ (-B_t) \tag{19}$$

$$F = \frac{q}{q_o} \tag{20}$$

Substituting Eq. (19) in Eq. (18)

$$1 - F = \frac{6}{\pi^2}(\exp -B_t)$$

or

$$B_t = -0.4977 - \ln(1 - F) \tag{21}$$

B_t values at different time for various initial concentrations are plotted in Fig. 6. It was observed that plots were linear but do not pass through origin confirming that, for the studied initial spent wash concentration, external mass transport mainly governs the sorption process. The D_i calculated using the relation

$$B_t = \frac{\pi^2 D_i}{r^2} \tag{22}$$

The D_i values were found to be 1.372×10^{-5}, 1.557×10^{-5}, 2.077×10^{-5}, 1.929×10^{-5} cm^2/s for an initial concentration of 2000, 5500, 8700 and 12500 mg/L, respectively.

The fitness of isotherm to the experimental equilibrium data was further analyzed using various non-linear error functions: χ^2, SSE, HYBRD, MPSD, ARE, and EABS. The values of error functions for different isotherms are given in Table 5. From the table Freundlich and Ho's pseudo-second order isotherm exhibits low values of non-linear error functions and high values of linear correlation coefficients that indicate that they seem to be the best fitting model for the experimental results.

Table 6
Thermodynamic constants calculated for sorption of spent wash onto fly ash using Freundlich isotherm

Temperature (K)	ΔG^0 (J/mol)	ΔH^0 (KJ/mol)	ΔS^0 (J/mol K)	r^2
293	−1574.67			
		−32.5487	105.0082	0.9875
303	−1173.23			
313	554.67			

3.5. Thermodynamic studies

The effect of temperature, a major factor influencing the sorption, was studied in the range of 293–313 K. Thermodynamic parameters ΔG^0, ΔH^0 and ΔS^0 were obtained from the experiments carried out at different temperatures as shown in Table 6. The ΔG^0 is the fundamental criterion to determine if a process occurs spontaneously. For a given temperature, a phenomenon is considered to be spontaneous if the ΔG^0 has a negative value. Moreover if ΔH^0 is positive, the process is endothermic and if it is negative, the process is exothermic. For the determination of ΔH^0 and ΔS^0, the relationship between sorption equilibrium constant K_T and Gibbs free energy was considered at any temperature:

$$\ln K_T = -\frac{\Delta G^0}{RT} = \frac{\Delta S^0}{R} - \frac{\Delta H^0}{RT} \tag{23}$$

The plot of $\ln K_T$ as a function of $1/T$ should give a linear relationship with slope of $\Delta H^0/R$ and an intercept of $\Delta S^0/R$. The negative values of ΔG^0 indicates spontaneous nature of sorption at lower temperature of 293 K and 303 K whereas a weak value at 313 K indicates that the process is feasible but non-spontaneous. The negative value of ΔH^0 indicates sorption process is exothermic occurs with release of heat. The positive value of ΔS^0 indicates that randomness of the system increases as sorption proceeds.

3.6. Design of batch sorption from isotherm data

Generally sorption processes proceed through varied mechanisms such as external mass transfer of solute onto sorbent followed by intraparticle diffusion. The empirical design procedures based on sorption equilibrium conditions are the most common method for predicting the adsorber size and performance. Sorption equilibrium is a dynamic concept achieved when the rate at which molecules adsorb onto a surface is equal to the rate at which they desorb. The physical chemistry involved may be complex and no single theory of sorption has been put forward to explain all the systems. The schematic diagram of single stage batch sorption system is shown in Fig. 7. The design objective is to reduce the color of spent wash of volume V (L) from an initial concentration of C_0 to C_1 (mg/L). The amount of adsorbent is M and the solute loading changes from q_o (mg/g) to q_1 (mg/g). At time $t = 0$, $q_0 = 0$ and

Table 5
Values of error functions for different isotherms for sorption of spent wash onto fly ash

Isotherm	Chi-square	SSE	HYBRD	MPSD	ARE	EABS	r^2
Freundlich	0.0102	0.5426	0.0101	0.0002	0.0252	1.293	0.9998
Langmuir	6.3012	345.2154	6.7853	0.2192	0.7311	30.121	0.9874
Temkin	2031.503	12534.45	174.603	2.8466	3.3541	196.710	0.9546
Lagergren's first order	52.2423	1783.579	30.2952	0.6707	1.5890	79.734	0.9003
Ho's second order	0.1152	8.096	0.1179	0.0021	0.0914	5.096	0.9962

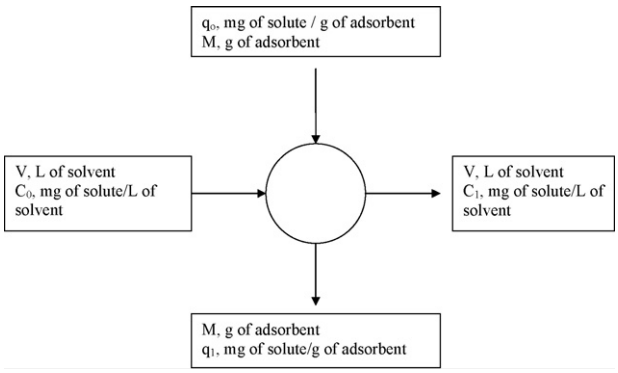

Fig. 7. Single stage batch adsorber design.

as time proceeds the mass balance equates the color removed from the spent wash to that picked up by the solid. The mass balance equation for the system can be given as [39]

$$V(C_0 - C_1) = M(q_0 - q_1) = Mq_1 \quad (24)$$

Under equilibrium conditions

$C_1 \rightarrow C_e$ and $q_1 \rightarrow q_e$

Since sorption isotherm studies fitted well to Freundlich isotherm, it is used for q_1 in equation batch adsorber design.

Rearranging Eq. (24)

$$\frac{M}{V} = \frac{(C_0 - C_e)}{q_1} = \frac{(C_0 - C_e)}{q_e} = \frac{(C_0 - C_e)}{K_f C_e^{1/n}} \quad (25)$$

Fig. 8 shows the plot between the predicted amounts of fly ash particles required to remove color of spent wash solutions of initial concentrations 5500 mg/L for 90, 80, 70 and 60% color removal at different solution volumes (1, 2, 3, 4, 5, 6, 7 L) for a single stage batch sorption system, for which the design procedure is outlined. For example, the amount of fly ash required for the 90% removal of color of spent wash solution of concentration 5500 mg/L was 135.7, 271.4, 407.1, 542.8, 678.5, 814.2 and 949.9 g for spent wash solution volumes of 1, 2, 3, 4, 5, 6 and 7 L, respectively.

3.7. Statistical analysis and modeling

The most important factors that affect the adsorption process are dilution (X_1), dosage of adsorbent (X_2) and temperature (X_3). In order to study the combined effect of these factors experiments were conducted at different combination of physical parameters. The results of the experimental design were studied and interpreted by MINITAB 14 statistical software to estimate the response of dependent variable. The range of the three variables studied is

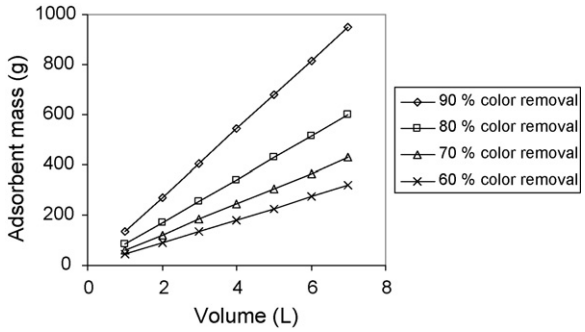

Fig. 8. Adsorbent mass (M) against volume of solution treated (V).

Table 7
Experimental range and levels of independent process variables

Independent variables	Low level (−1)	High level (+1)
Dilution (%)	5	20
Dosage of adsorbent (g)	2	14
Temperature (K)	293	313

shown in Table 7. The experimental results obtained for 2^3 full factorial designs and the corresponding fit and residuals are given in Table 8. Decolorization yield varied within 56–93%. The decolorization yield (Y_1) can be predicted from regression coefficients as [42,43].

$$Y_1 = 74.928 - 2.856X_1 + 14.303X_2 - 0.948X_3 + 1.024(X_1X_2) + 0.774(X_1X_3) \quad (26)$$

The students t-test and Fischer F-test was used to determine the significance of the regression coefficients of the parameters. The P-values were used as a tool to check the significance of each of the interaction among the variables. More significant the terms of coefficient if value of 't' is larger and value of 'P' is smaller [44,45]. The effect of dosage of adsorbent was very effective with large t-value (70.97) and small P-value of zero.

For color removal the two-way interactions of dilution and dosage of adsorbent ($P = 0.037$), dilution and temperature ($P = 0.062$) were found statistically significant. The statistical significance of ratio of mean square due to regression and mean square residual error was tested using ANOVA test. It is a statistical technique that subdivides the total variation in a set of data into component parts associated with specific sources of variation for the purpose of testing hypotheses on the parameter of the model [46]. According to the ANOVA, F values for main effects are very large and that of two-way interactions are high indicate that most of the variation in the response can be explained by the regression equation. The ANOVA chart for color removal is shown in Table 9. The coefficient of determination for color removal ($r^2 = 0.9996$) implies that 99.96% of the sample variation for color removal is explained by the independent variables and this also means that the model did not explain only about 0.04% of sample variation for color removal. The optimization of decolorization was done against the set target of 95% color removal. The optimal removal of color of 93% was obtained for dilution (5%), dosage of adsorbent (10 g) and temperature (293 K). The actual color removal at optimal conditions was 92.24%, which confirms close to factorial design results.

3.8. Adsorption studies in packed column

Bed depth service time model is a simple model that assumes a linear relationship between bed height and service time of a column [47]. The model is represented as

$$t_b = \frac{N_0 Z}{C_0 U_0} - \frac{1}{K_a C_o} \ln\left(\frac{C_0}{C_b} - 1\right) \quad (27)$$

The model ignores the intraparticle mass transfer resistance and external film resistance such that adsorbate is adsorbed onto the adsorbent surface directly. The effect of bed height as studied at constant flow rate (1 L/h) and initial concentration of spent wash (2000 mg/dm^3). Breakthrough concentration was taken as $0.1C_0$ (200 mg/dm^3) and corresponding time was taken as column service time (t_b). Fig. 9 shows the breakthrough curves at different bed heights 5, 10, 15 and 20 cm. Breakthrough and exhaustion time increased with increase of bed height due to increase in surface area of fly ash available for adsorption. The sharp leading edges of the breakthrough curves at low residence time indicate the poor utilization of the column capacity. Plot of service time versus bed

Table 8
Experimental data, fits and residuals

Run	Dilution (%) X_1	Dosage of adsorbent (g) X_2	Temperature (K) X_3	%Color removal Y_1	Fit for color removal	Residuals for color removal
1	5	14	293	92.562	92.7835	−0.2215
2	5	2	313	62.562	62.7835	−0.2215
3	20	2	313	56.235	56.5718	−0.3368
4	5	14	313	89.562	89.3405	0.2215
5	20	14	293	87.236	87.5728	−0.3368
6	20	2	293	57.256	56.9193	0.3367
7	20	14	313	87.562	87.2253	0.3367
8	5	2	293	66.448	66.2265	0.2215

Table 9
Analysis of variance for %color removal

Source	DF	Seq SS	Adj SS	Adj MS	F	P
Main effects	3	1708.94	1708.94	569.647	1753.16	0.001
Two-way interactions	2	13.18	13.18	6.591	20.28	0.047
Residual error	2	0.65	0.65	0.325		
Total	7	1722.77				

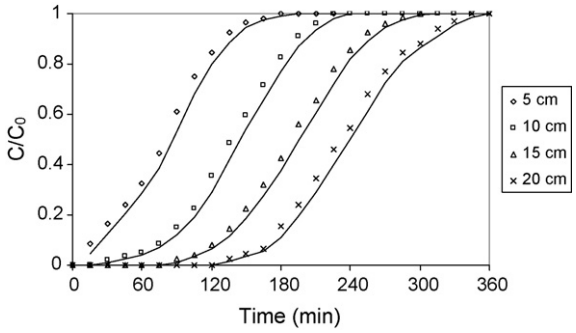

Fig. 9. Breakthrough curves for continuous sorption of spent wash onto fly ash at different bed heights.

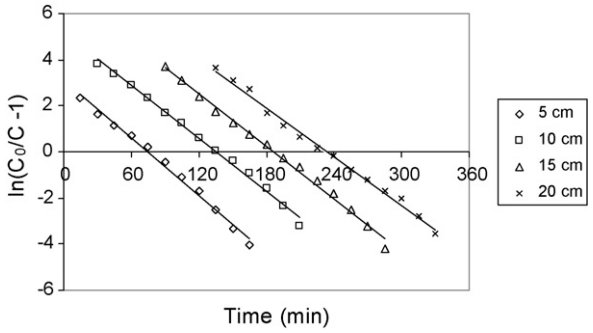

Fig. 10. Thomas model for continuous model of sorption of spent wash onto fly ash at different bed height.

height (not shown) was linear ($r^2 = 0.9966$). The sorption capacity of the bed per unit volume of the bed ($N_0 = 196.248$ g/L) and rate constant ($K_a = 3.99 \times 10^{-5}$ L/mg min) were calculated from the slope and intercept of the plot, respectively.

Successful design of a column adsorption process requires prediction of the concentration–time profile or breakthrough curve for the effluent. The Thomas model is widely used to study the column performance for adsorption process. The Thomas model assumes Langmuir kinetics of adsorption and no axial dispersion and that the rate driving force obeys second order reversible reaction kinetics. The model is represented as [48]:

$$\frac{C}{C_0} = \frac{1}{1 + \exp\ [(K_{Th}/Q)(q_0 M - C_0 V_{eff})]} \tag{28}$$

The linearized form represented by

$$\ln\left(\frac{C_0}{C}\right) = \frac{(K_{Th} q_0 M)}{Q} - \frac{(K_{Th} C_0 V_{eff})}{Q} \tag{29}$$

Effluent volume is calculated from following equation

$$V_{eff} = Q t_{total} \tag{30}$$

$$\ln\left(\frac{C_0}{C}\right) = \frac{(K_{Th} q_0 M)}{Q} - (K_{Th} C_0 t_{total}) \tag{31}$$

The K_{Th} and q_0 are calculated from the slopes and intercepts obtained from Fig. 10 and are tabulated in Table 10. The linearized Thomas equation adequately describes the experimental break through sorption data as evident from the values obtained by the model.

The Adams–Bohart model is used for the description of the initial part of breakthrough curve. This model assumes that the adsorption rate is proportional to both the residual capacity of the sorbent and the concentration of the sorbing species [48].

$$\ln\left(\frac{C}{C_0}\right) = K_{AB} C_0 t - \frac{(K_{AB} N_0 Z)}{U_0} \tag{32}$$

From the plot of $\ln C/C_0$ against time at a given bed height and flow rate values describing the characteristic operational parameters of the column can be determined.

The Adams–Bohart sorption model is applied to the continuous sorption of spent wash onto fly ash in the packed bed column for the description of initial part of breakthrough curve using the

Table 10
Thomas model for the continuous sorption of spent wash

Bed height (cm)	Equilibrium specific uptake of spent wash solids q_0 (mg/g)	Kinetic constant in the Thomas model K_{Th} (ml/mg min)	r^2
5	414.722	0.0209	0.9922
10	376.032	0.0190	0.9948
15	345.013	0.0190	0.9937
20	325.377	0.0176	0.9935

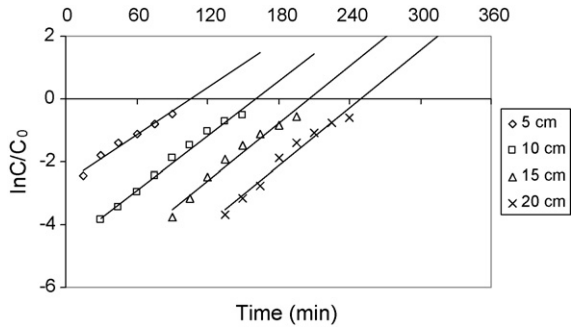

Fig. 11. Adams–Bohart model for continuous sorption of spent ash onto fly ash at different bed height.

experimental data. A linear relationship between $\ln C/C_0$ and t was obtained for the initial part of the breakthrough curve up to 50% breakthrough for all bed heights and is shown in Fig. 11.

4. Conclusion

The present study shows that the fly ash, a by-product of coal-fired power stations can be used as an adsorbent for the removal of color from distillery spent wash. The Freundlich and pseudo-second order kinetics model were observed to represent the sorption data perfectly. External mass transfer controlled the color removal at earlier stages and intraparticle diffusion at later stages of sorption. A Boyd plot confirms that the external mass transfer was the slowest step involved in the sorption process. The continuous sorption was found to closely represent the Thomas model for different bed height studies. Adams–Bohart model was found to represent closely the initial part of the breakthrough curve.

References

[1] B. Kannabiran, A. Prakasam, Effect of distillery effluent on seed germination, seedling growth and pigment content of Bigna Mungo Hepper (C.V.T.9), GEOBIOS 20 (1993) 108–112.
[2] C.S. Agarwal, G.S. Pandey, Soil pollution by spent wash discharge: Depletion of manganese (II) and impairment of its oxidation, J. Environ. Biol. 15 (1994) 49–53.
[3] F.J. FitzGibbon, P. Nigam, D. Singh, R. Marchant, Biological treatment of distillery waste for pollution remediation, J. Basic Microbiol. 35 (1995) 93–301.
[4] B.L. Wedzicha, M.T. Kaputo, Melanoidins from glucose and glycine: composition, characteristics and reactivity towards sulphite ion, Food Chem. 43 (1992) 359–367.
[5] V. Kumar, L. Wati, P. Nigam, I.M. Banat, B.S. Yadav, D. Singh, R. Marchant, Decolorization and biodegradation of anaerobically digested sugarcane molasses spent wash effluent from biomethanation plants by white rot fungi, Process Biochem. 33 (1) (1998) 83–88.
[6] P. Manisankar, C. Rani, S. Viswanathan, Effects of halides in the electro chemical treatment of distillery effluent, Chemosphere 57 (8) (2004) 961–966.
[7] D. Francisca Kalavathi, L. Uma, G. Subramanian, Degradation and metabolization of the pigment-melanoidin in distillery effluent by the marine cyanobacterium *Oscillatoria boryana* BDU 92181, Enzyme Microb. Technol. 29 (2001) 246–251.
[8] S. Ohmomo, Y. Kancko, S. Sirianuntapiboon, P. Somchai, P. Atthasampunna, I. Nakamura, Decolorization of molasses wastewater by a thermophileic strain, *Aspergillus fumigatus* G-2-6, Agric. Biol. Chem. 51 (1987) 3339–3346.
[9] V. Kumar, L. Wait, F. Fitzgibbon, P. Nigam, I.M. Bansat, D. Singh, R. Marchant, Bioremediation and decolorization of anaerobically digested distillery spent wash, Biotechnol. Lett. 19 (1997) 285–289.
[10] A.P. Thakkar, V.S. Dhamankar, B.P. Kapadnis, Biocatalytic decolourisation of molasses by *Phanerochaete chrysosporium*, Bioresour. Technol. 97 (1988) 1377–1381.
[11] G. Christoskovas, L.D. Lazarov, Electrochemical method for purification and discoloration of cellulose paper industry wastewaters, Environ. Prot. Eng. 14 (3–4) (2006) 69–76.
[12] P. Manisankar, S. Viswanathan, C. Rani, Electrochemical treatment of distillery effluent using catalytic anodes, Green Chem. 5 (2003) 270–274.
[13] P.K. Chaudhari, I.M. Mishra, S. Chand, Decolorization and removal of chemical oxygen demand (COD) with energy recovery: treatment of biodigester effluent of a molasses-based alcohol distillery using inorganic coagulants, Colloid Surf. A 296 (2007) 238–247.
[14] V.P. Migo, M. Matsumure, E.J.D. Rosarto, H. Kataka, Decolouration of molasses wastewater using an inorganic coagulates, J. Ferment. Bioeng. 75 (6) (1993) 438–442.
[15] S. Sinha, Y. Yoon, G. Amy, J. Yoon, Determining the effectiveness of conventional and alternative coagulants through effective characterization schemes, Chemosphere 57 (2004) 1115–1122.
[16] J.E. Van Benschoten, J.K. Edzwald, Measuring aluminum during water treatments, J. Am. Water Works Assoc. 82 (1990) 71–78.
[17] Z. Song, C.J. Williams, R.G.J. Edyvean, Treatment of tannery wastewater by chemical coagulation, Desalination 164 (2004) 249–259.
[18] R.G. Miller, F.C. Kopfler, K.C. Kelty, J.A. Stober, N.S. Ulmer, The occurrence of aluminum in drinking water, J. Am. Water Works Assoc. 76 (1984) 84–91.
[19] F.B. Dilek, S. Bese, Treatment of pulping effluents by using alum and clay-Color removal and sludge characteristics, Water SA 27 (3.) (2001).
[20] M.L. Hall, W.R. Livingston, Fly ash quality, past, present and future, and the effect of ash on the development of novel products, J. Chem. Technol. Biotechnol. 77 (2002) 234–239.
[21] V.S. Mane, I.D. Mall, V.C. Srivastava, Use of bagasse fly ash as an adsorbent for the removal of brilliant green dye from aqueous solutions, Dyes Pigments 73 (2007) 269–278.
[22] S. Wang, Y. Boyjoo, A. Choueib, A comparative study of dye removal using fly ash treated by different methods, Chemosphere 60 (2005) 1401–1407.
[23] K.V. Kumar, V. Ramamurthi, S. Sivanesan, Modeling the mechanism involved during the sorption of methylene blue onto fly ash, J. Colloid Interface Sci. 284 (2005) 14–21.
[24] S. Kara, C. Aydiner, E. Demirbas, M. Kobya, N. Dizge, Modeling the effects of adsorbent dose and particle size on the adsorption of reactive textile dyes by fly ash, Desalination. 212 (2007) 282–293.
[25] V. Ponnusami, V. Krithika, R. Madhuram, S.N. Srivastava, Biosorption of reactive dye using acid treated rice husk: factorial design analysis, J. Hazard. Mater. 142 (2007) 397–403.
[26] Y. Bulut, H. Aydin, A kinetics and thermodynamics study of methylene blue adsorption on wheat shells, Desalination 194 (2006) 259–267.
[27] G. McKay, E.I. Geundi, M.M. Nasser, Equilibrium studies during the removal of dyestuff from aqueous solutions using bagasse pith, Water Res. 21 (1987) 1513–1518.
[28] W.R. Knocke, L.H. Hemphill, Mercury (II) sorption of waste rubber, Water Res. 15 (1981) 275–282.
[29] A.G. Rowley, A. Cunningham, F.M. Husband, Mechanisms of metal adsorption from aqueous solutions by waste tyre rubber, Water Res. 18 (1984) 981–984.
[30] APHA, Standard methods for the examination of water and wastewater, 20th ed., American public health Association, American Water Works Association and Water pollution Control Federation (1998) Washington D.C.
[31] C. Raghukumar, G. Rivonkar, Decolorization of molasses spent wash by the white rot fungus *Flavodon flavus*, isolated from a marine habitat, Appl. Microbiol. Biotechnol. 55 (2001) 510–514.
[32] G. Annadurai, R.Y. Sheeja, S. Mathalai Balan, T. Murugesan, V.R. Srinivasamoorthy, Factorial design of experiments in the determination of adsorption equilibrium constants for basic methylene blue using biopolymer, Bioprocess Eng. 20 (1999) 37–43.
[33] G. Annadurai, Design of optimum response surface experiments for adsorption of direct dye on chitosan, Bioprocess Eng. 23 (2000) 451–455.
[34] Y.S. Ho, J.F. Porter, G. McKay, Equilibrium isotherm studies for the sorption of divalent metal ions onto peat: copper, nickel and lead single component systems, Water Air Soil Poll. 141 (2002) 1–33.
[35] A. Jumasiah, T.G. Chuah, J. Gimbon, T.S.Y. Choong, I. Azni, Adsorption of basic dye onto palm kernel shell activated carbon sorption equilibrium and kinetic studies, Desalination 186 (2005) 57–64.
[36] H.M.F. Freundlich, Over the adsorption in solution, J. Phys Chem. 57 (1906) 385–470.
[37] I. Langmuir, The adsorption of gases on plane surface of glass, mica and platinum, J. Am. Chem. Soc. 40 (1916) 1361–1368.
[38] C. Aharoni, M. Ungarish, Kinetics of activated chemisorption. Part 2. Theoretical models, J. Chem. Soc. Faraday Trans. 73 (1977) 456–464.
[39] V. Vadivelan, K. Vasanth Kumar, Equilibrium, kinetics, mechanism and process design for the sorption of methylene blue onto rice husk, J. Colloid Interface Sci. 286 (2005) 90–100.
[40] Y.S. Ho, G. Mckay, The kinetics of sorption of divalent metal ions onto sphagnum moss peat, Water Res. 34 (3) (2000) 735–742.
[41] Y.S. Ho, G. McKay, Pseudo second order model for sorption process, Process Biochem. 34 (1999) 451–465.
[42] M. Elibol, Response surface methodological approach for inclusion of perfluorocarbon in actinohordin fermentation medium, Process Biochem. 38 (2002) 667–773.
[43] K. Ravikumar, S. Krishnan, S. Ramalingam, K. Balu, Optimization of process variables by application of response surface methodology for dye removal using a novel adsorbent, Dyes pigments 72 (1) (2007) 66–74.
[44] M.M.D. Zulkali, A.L. Ahmad, N.H. Norulakmal, *Oryza sativa* L. husk as heavy metal adsorbent: optimization with lead as model solution, Bioresour. Technol. 97 (2006) 21–25.
[45] K. Ravikumar, S. Ramalingam, S. Krishnan, K. Balu, Application of response surface methodology to optimize the process variables for reactive red and

acid brown dye removal using a novel adsorbent, Dyes Pigments 70 (1) (2006) 18–26.
[46] H.M. Kim, J.G. Kim, J.D. Cho, J.W. Hong, Optimization and characterization of UV-curable adhesives for optical communication by response surface methodology, Polym. Test. 22 (2003) 899–906.
[47] C.K. Danny, J.F. Porter, G. McKay, Optimized correlations for the fixed bed adsorption of metal ions on bone char, Chem. Eng. Sci. 55 (2000) 5819–5829.
[48] B. Preetha, T. Viruthagiri, Batch and continuous biosorption of chromium (VI) by *Rhizopus arrhizus*, Sep. Purif. Technol. 57 (2007) 126–133.